

## LARGE EDDY SIMULATION OF BUOYANT PLUMES

Worthy J., Rubini P.A.

School of Engineering, Cranfield University, Cranfield, Bedfordshire, MK43 OAL, UK

### ABSTRACT

The use of Computational fluid dynamics (CFD) is increasingly being employed to investigate internal building flows, for heating, ventilation, and fire safety, where buoyancy effects due to thermal gradients become significant. Conventional CFD approaches have, in the past, been largely based upon a Reynolds Averaged form of the governing Navier-Stokes equations (RANS), often in a steady state form. With the increasing power and accessibility of computer resources an alternative modelling strategy is becoming a viable possibility. Large Eddy Simulation (LES) attempts to capture the significant, energy containing, scales of the turbulent fluctuations, whilst modelling only the smaller scales. LES models still rely on empirical closure to model the unresolved sub-grid scale (SGS) stresses, an 'SGS-model', which, despite claims to the contrary, can often be of considerable importance. In this paper a selection of static and dynamic LES SGS-models for both the sub-grid stresses and scalar fluxes are assessed for a non-combusting turbulent plume. The results clearly demonstrate that choice of SGS-model can make a significant difference to the resulting flow averages with the dynamic models performing most realistically.

### NOMENCLATURE

Fr	Froude number	$\phi$	molecular stress term
g	gravity	$\kappa$	wavenumber
k	thermal conductivity	$\Pi$	reduced pressure term
L	Leonard term	$\rho$	density
Pr	Prandtl number	$\tau_{ij}$	stress tensor
$q_j$	subgrid flux	$\nu$	kinematic viscosity
Re	Reynolds Number		
t	time		
T	temperature		
$T_{ij}$	test-filter scale stress		
u	velocity		
X/Y/Z	Cartesian axes (Y vertical)		

### Greek Letters

$\delta_{ij}$	Kronecker delta
$\Delta$	filter width, grid width
$\varepsilon$	temperature difference, dissipation term

### Subscripts

$i,j,k$	component direction
$0$	initial / input value
$t$	turbulent value

### Superscripts

$\bar{X}$	filtered variable, Favre averaged variable
$\tilde{X}$	Favre averaged variable

### INTRODUCTION

Large eddy simulation is an increasingly viable option for turbulence modelling, providing an alternative to the established RANS approach. Since the early work of Smagorinsky [1], Lilly [2,3], Deardorff [4], Schumann [5], and Leonard [6]) the development of computing power has grown and allows for LES requirements in an increasing variety of flows. The development of LES has been primarily concerned with the development of models for the incompressible Navier-Stokes equations, with relatively little development of the flux models needed for the filtered Boussinesq or low Mach number (LMN) equations.

The models which have been developed have been typically tested against either the original Smagorinsky model, Zang et al. [7], or against the dynamic Smagorinsky model, Cottet and Vasilyev [8], but there has been little work providing a comprehensive overview of the relative merits and limitations of the different models, particularly in non-isothermal incompressible flows, with the notable exceptions of Bastiaans et al. [9] and Peng and Davidson [10]. This work follows in a similar spirit by investigating different sub-grid models for both the stresses and more importantly, for buoyant flows, for the scalar fluxes where development has lagged behind that of the sub-grid stress models. Non-combusting buoyant plumes were selected to eliminate any modelling errors related to the combustion process itself.

It is clearly the case that for the application of LES to practical flows to be useful, the sub-grid models must be sufficient for the required purposes, and that further models, including combustion models, will be limited in their accuracy to that of the underlying turbulence model and numerical truncation error. Significant flaws in the simple eddy viscosity based models have been found, concerning accuracy, laminar regions and backscatter, yet they are still the most used models in applications. An often quoted defence of this is that the choice of sub-grid scale model should not significantly affect the overall flow. Unfortunately for buoyant plumes this does not appear to be the case, as will be shown herein.

## GOVERNING EQUATIONS

The Low Mach Number (LMN) equations have been proposed for incompressible flows with heat transfer and combustion, rather than the more restricted Boussinesq equations, where the density variations are assumed to be small and only incorporated in the buoyant term. The LMN equations were derived by Rehm and Baum [11], and Paulucci [12]. The filtered continuity, momentum, and temperature equations are based on these, following Germano [13], where a reduced equation of state is also employed.

$$\frac{\partial \bar{\rho}}{\partial t} + \frac{\partial \bar{\rho} \tilde{u}_i}{\partial x_i} = 0 \quad (1)$$

$$\frac{\partial \bar{\rho} \tilde{u}_i}{\partial t} + \frac{\partial \bar{\rho} \tilde{u}_i \tilde{u}_j}{\partial x_j} = -\frac{\partial \bar{\Pi}}{\partial x_i} + \frac{1}{\text{Re}} \frac{\partial^2 \tilde{u}_i}{\partial x_j^2} + \frac{1}{Fr} (\bar{\rho} - 1) g_i - \frac{\partial \bar{\rho} \tau_{ij}}{\partial x_j} \quad (2)$$

$$\frac{\partial \tilde{T}}{\partial t} + \tilde{u}_j \frac{\partial \tilde{T}}{\partial x_j} = \frac{1}{\bar{\rho}} \frac{1}{\text{Re Pr}} \frac{\partial^2 \tilde{T}}{\partial x_j^2} - \frac{\partial q_j}{\partial x_j} \quad (3)$$

The time-dependent pressure term in the temperature equation is assumed to be negligible when open plume boundaries are employed. A reduced pressure term appears in the momentum equations, where the acoustic waves have been filtered out and the hydrostatic buoyancy term has been incorporated.

## LES SUB-GRID SCALE MODELS

The sub-grid stress and scalar flux terms appearing in equations (2) and (3), equation (4), and flux terms, equation (5), must of course be modelled. As is common practice, models developed for incompressible flows are used equivalently for the Favre averaged stresses and fluxes. Note, for notational purposes, the over bar is used in place of the tilde from now on.

$$\tau_{ij} = \overline{u_i u_j} - \bar{u}_i \bar{u}_j \quad (4)$$

$$q_j = \overline{u_j T} - \bar{u}_j \bar{T} \quad (5)$$

In an analogous procedure to that adopted by RANS simulations, the sub-grid stresses may be related to the strain rate through an empirical eddy-viscosity, and similarly the standard gradient diffusion model (SGDH) employed for the scalar fluxes.

$$\tau_{ij} = -2\nu_t \bar{S}_{ij} \quad (6)$$

$$q_j = \frac{\nu_t}{Pr_t} \frac{\partial T}{\partial x_j} \quad (7)$$

Equation (6) gives the generic form of the eddy viscosity models, any form of which provides the basis for the SGDH model in Equation (7).

The Smagorinsky sub-grid scale model, Smagorinsky [1], in common RANS nomenclature, may be considered to be a so-called mixing length model. Where the mixing length is based upon the filter width,  $\Delta$ .

$$\nu_t = C\Delta^2 |\bar{S}|, \quad |\bar{S}| = (2\bar{S}_{ij}\bar{S}_{ij})^{1/2} \quad (8)$$

The Smagorinsky model constant takes a theoretical constant of approximately 0.03 in the above formulation, but 0.01 has been recommended, Lilly [3]. This has been the most widely used model since its inception, and remains so today, despite its limitations. Most significantly of these are propensities to display bad a priori correlations, showing low accuracy, and non-zero values in laminar flows. The model is used, however, as it does dissipate the turbulent energy successfully, which is the most important quality.

Analogously to RANS models, sub-grid scale transport models have also been developed. Schumann [5] developed a full second moment transport method for LES (transport equations for each of the stresses and fluxes), however these have not been used due to their high computational costs, and arguably unnecessary complexity. However, one equation models (for example, Horiuti,[14]) in which the sub-grid kinetic energy is transported, have been developed and applied, although not to the same extent as the Smagorinsky models. This model is also based upon the eddy viscosity concept, where the length scale is again taken to be the filter width and the time scale to be related to the sub-grid turbulent kinetic energy.

$$\nu_t = C_m \Delta k^{1/2} \quad (9)$$

The constant has been theoretically found to be 0.07, Sagaut [15], although values ranging between 0.04 and 1 have been used, Schmidt and Schumann [16]. The transport equation may be expressed as,

$$\frac{\partial k}{\partial t} + \bar{u}_j \frac{\partial k}{\partial x_j} = \nu \frac{\partial^2 k}{\partial x_j^2} - \frac{k^{3/2}}{\Delta} - \tau_{ij} \frac{\partial \bar{u}_i}{\partial x_j} \quad (10)$$

The dissipation term is modelled as given by Lilly [2,3]. A further diffusion term has been neglected, following Davidson [17].

The generalised gradient diffusion model (GGDH), was presented for RANS modelling by Daly and Harlow [18] as an alternative to the SGDH model, and has subsequently been shown to be a significant improvement for plume simulations, Sanderson [19], Worthy et al. [20]. With minor alterations it can easily be adopted in LES simulations with the following formulation.

$$q_j = -c_t \Delta k^{-0.5} \tau_{jk} \frac{\partial T}{\partial x_k} \quad (11)$$

This formulation requires the use of the sub-grid kinetic energy transport equation again, although this could be calculated from the stresses and substituted instead. A constant value of 5 has been employed in this work after initial tests, although a final recommended value has yet to be determined.

Germano et al. [21] introduced dynamic modelling, using the Germano relation [13]. This concept is applicable to all models with empirically determined constants, replacing the constant by a variable evaluated locally in space and time. Equation (12) is the essential relation, which relates different filtered levels of the governing equations.

$$T_{ij} = \overrightarrow{\tau}_{ij} + L_{ij} \quad (12)$$

$$T_{ij} = \overleftrightarrow{u_i u_j} - \overleftrightarrow{\bar{u}_i \bar{u}_j} \quad (13)$$

$$\tau_{ij} = \overline{u_i u_j} - \bar{u}_i \bar{u}_j \quad (14)$$

$$L_{ij} = \overleftrightarrow{\bar{u}_i \bar{u}_j} - \overleftrightarrow{\bar{u}_i \bar{u}_j} \quad (15)$$

Equation (13) defines the stress of the double filtered (normally termed test-filtered since the same filter is not necessary) governing equations, equation (14) is the original sub-grid stress, and equation (15) is a directly calculable term (the Leonard term) from the single-filtered variables. Substituting an arbitrary model with a constant into equations (13) and (14), equation (12) can be rewritten with the following.

$$Cf(\overrightarrow{\bar{u}_i}) = \overrightarrow{Cf(\bar{u}_i)} + L_{ij} \quad (16)$$

Equation (16) rearranged and following Lilly [22] gives an explicit formula for the constant.

$$C = \frac{1}{2}(L_{ij}M_{ij} / M_{kl}M_{kl}) \quad (17)$$

Where  $M_{ij}$  is a function dependent on the choice of the sub-grid model. Substitution of the Smagorinsky model yields equation (18), which may now be evaluated.

$$M_{ij} = (-2\Delta^2 \overleftrightarrow{\bar{S}} \overleftrightarrow{\bar{S}}_{ij} + 2\Delta^2 \overleftrightarrow{\bar{S}} \overleftrightarrow{\bar{S}}_{ij}) \quad (18)$$

The dynamic SGDHD model can be evaluated in a similar manner.

## NUMERICAL METHOD

In the present work a reduced form of the projection method introduced by Najm et al. [23] was employed. The method is 2<sup>nd</sup> order accurate in time, but only the first step of the two-step method was found to be necessary. This does not affect the formal accuracy of the overall scheme. A 3<sup>rd</sup> order upwind scheme was employed for the momentum convection terms and a 2<sup>nd</sup> order TVD scheme, Sweby [24], employed for the temperature convection. Central difference, 2<sup>nd</sup> and 4<sup>th</sup> order schemes were used for the respective diffusion terms, and the pressure term was calculated with a 2<sup>nd</sup> order central scheme. The algorithm was implemented for parallel computation using MPI, and the pressure Poisson equation solved using a fast multigrid technique.

At the plume source some form of instability has been found to be necessary to initiate a turbulent flow. Two techniques were adopted. Firstly, a structured instability, given by Equation (24) in which two modes are used.

$$v' = AV(r) \sum_{n=1}^2 \sin(2\pi ft / n + \theta) \quad (24)$$

Where,  $A$ , is the fraction of the inlet velocity, 0.2,  $V(r)$ , is the inlet velocity as a function of radius,  $f$ , is the frequency constant, 0.3,  $t$  is time, and  $\theta$  is the angle from the centre of the source. These disturbances are enhanced by strong random strength and random duration fluctuations across the inlet, with a maximum of 0.35, and a maximum duration of 100 time steps.

## RESULTS

The experiment of Shabbir and George [25] has been simulated, with similar solution parameters to Zhou et al. [26]. In the experiment a jet of heated air entered a 2m x 2m x 5m high enclosure through a 6.35cm diameter nozzle, at a velocity of  $0.98\text{ms}^{-1}$  and a temperature of 292 C.

Approximately half-million grid points were used, on a uniform mesh of  $63 \times 127 \times 63$  with a resolution such that the width of the source was represented by 9 cells. The non-dimensionalisation was based upon the inflow velocity and the source width, giving a source of 1 unit diameter, and inflow velocity of 1 unit, resulting in a domain of  $7 \times 14.11 \times 7$  unit volume. The ambient temperature was assumed to be 300K and the inlet temperature of the jet to be 567K, yielding,  $\varepsilon$ , the temperature difference between the ambient and the inlet, a non-dimensional value of 0.893. The Reynolds number was defined to be equal to 1300 and the Froude number defined to be equal to 1.54.

The aim of this work is to highlight the differences between different LES models, and to show that choice of LES model can make a significant difference to the resulting flow averages, and to present the models in such a way as to better understand their behaviour. In support of this aim a control simulation was also obtained with no sub-grid model.

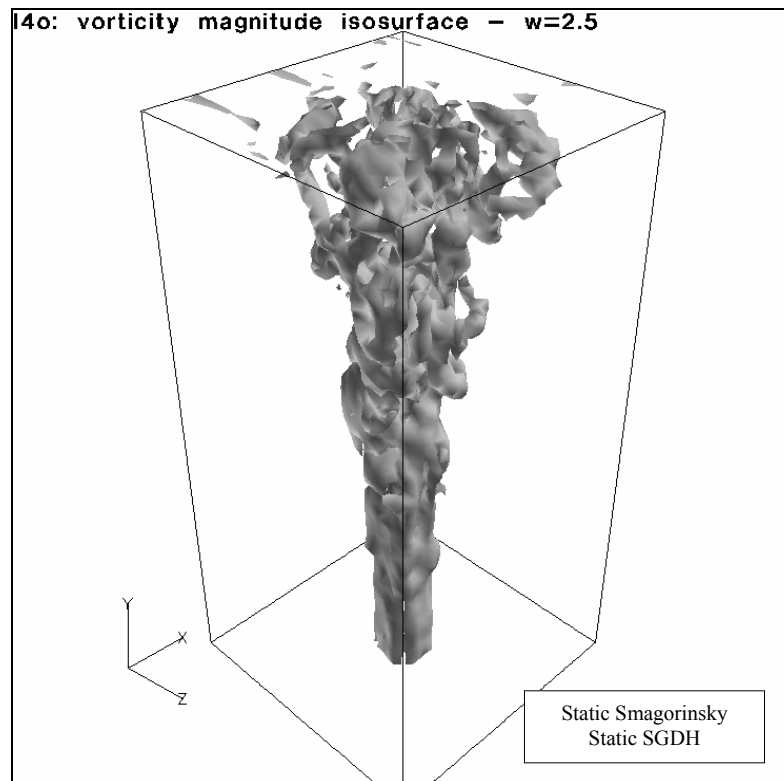


Figure 1. Isosurface of vorticity magnitude

An instantaneous snapshot of a typical simulation is given in figure 1, showing an isosurface of vorticity. The flow is laminar at the inlet, although the instabilities can be seen, the transition region can be seen, and fully developed turbulence is achieved towards the top of the domain.

The time spectra are plotted for the Smagorinsky model simulation in figure 2. The turbulent kinetic energy is shown to have a slightly higher gradient at this point than the typical Kolmogorov  $-5/3$

gradient, but is sufficiently similar to indicate a fully turbulent flow. The individual components, the spectra of the horizontal and vertical velocity fluctuations, demonstrate that the turbulence is very nearly isotropic by this point. Spectra plots taken at an earlier stage in transition show much stronger anisotropy in the spectra and further along show the spectra to be fully isotropic.

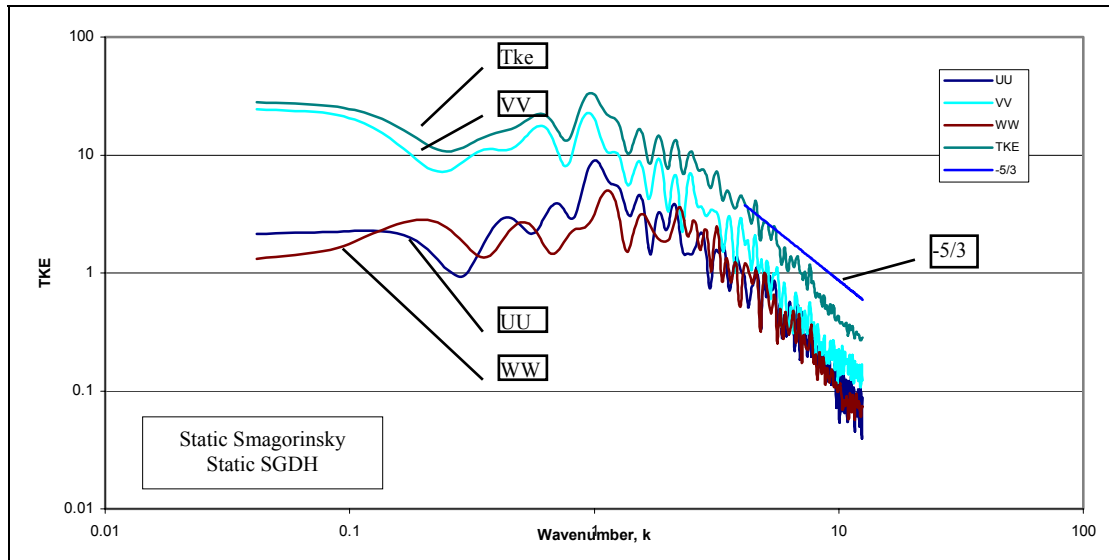


Figure 2. Time spectra for the turbulent kinetic energy and its component parts, on the plume centreline

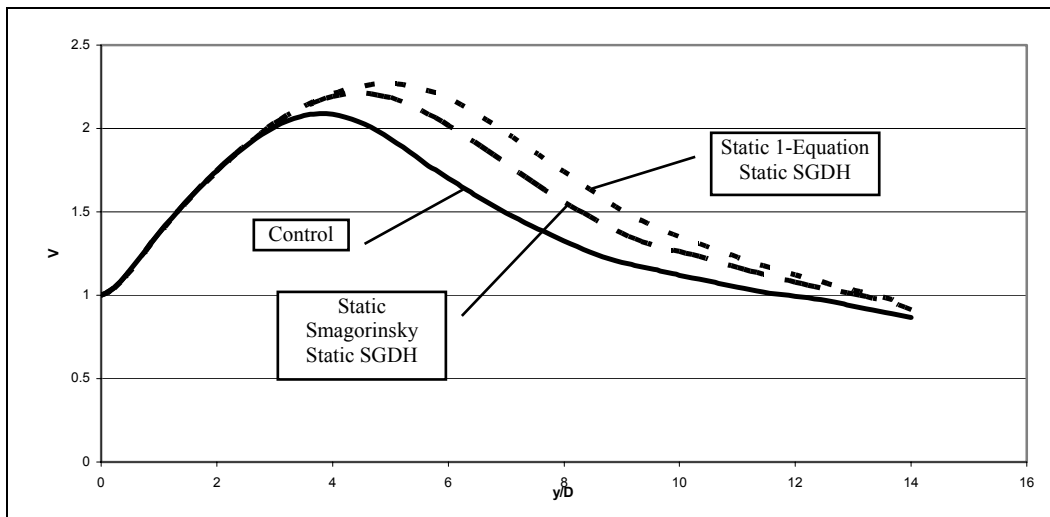


Figure 3. Velocity decay along plume centreline

The sub-grid stresses and fluxes have a significant effect with respect to the control simulation. This is clearly evident from the centreline velocity decays plotted in Figure 3, in which the one equation model in conjunction with the SGDH flux model has largest maximum magnitude followed by the fastest decay rate. The peak velocity roughly indicates the onset of transition, which then develops in the initially swift decay, before the slower decay rate indicating a near full transition to turbulence (at the beginning of this region the inertial subrange is only nearly isotropic, whereas it is fully isotropic by the end of the domain).

The difference between the Smagorinsky and one equation sub-grid models is demonstrated through consideration of the main centreline stress, the vertical normal stress,  $T_{22}$  (Figure 4), (although it is the radial stress which has the highest peak away from the centreline for the eddy stresses). The magnitudes are reflective of the strength of the turbulent viscosities which governs the strength of all the stress (and eddy flux) terms. In the laminar region where the instabilities are growing the one equation model has the greater magnitude (although not at the very start, due to a negligible magnitude inflow boundary condition), damping the transition more quickly. The subsequent increase in the stress magnitude in the transitional region is disproportionate to the increase in the centreline velocity, further showing the greater dissipation of the one equation model. Horiuti [14] found the Smagorinsky model to be the more dissipative of the two eddy stress models using a model constant of 0.05 instead of 0.07, and the same constants in the sub-grid energy equation. Adjusting the model constants obviously affects the level of dissipation.

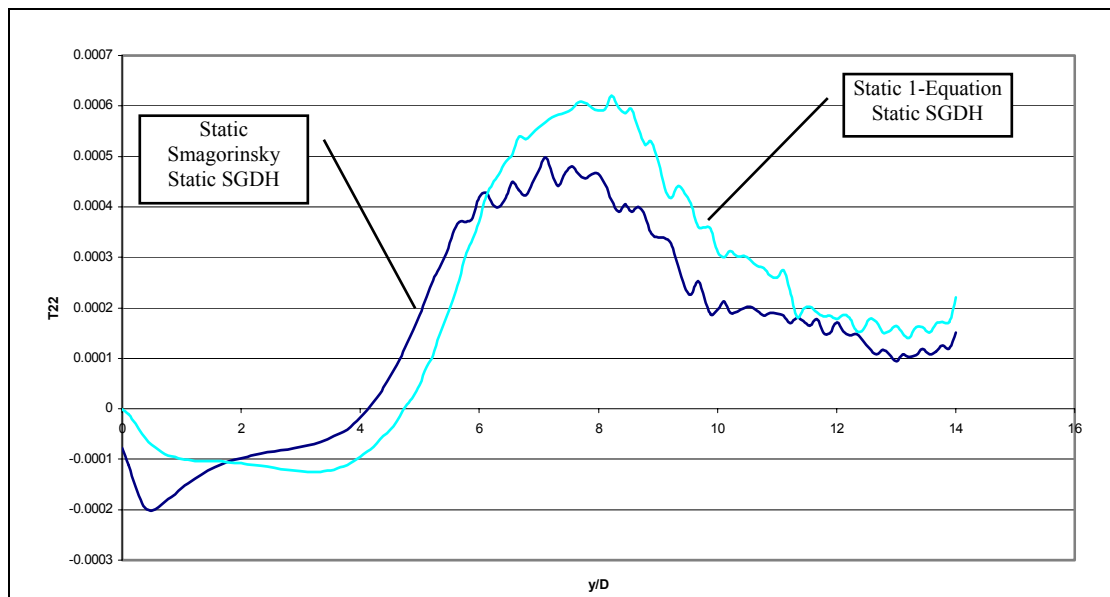


Figure 4. Vertical normal stress,  $T_{22}$ , along plume centreline

The sub-grid stress models are relatively well developed, but the sub-grid scalar flux models are much less so. The influence of the SGS flux model is shown in the following section with simulations using the one equation stress model, with the SGDH model, the GGDH model, or no flux model.

The effect of the flux model is shown to be the dominant term in the case of the SGDH model, see Figure 5. The difference in maximum velocity between the control simulation and that with the one equation stress model is much less than the difference between that with the one equation stress model and the one equation stress with SGDH flux model. The GGDH model is more dissipative than without, and also leads to a higher decay rate, but not by much. It is worth noting at this point the effect of the numerical scheme, which can be diffusive. It is necessary to ensure that all models can be tested against each other, but implicitly numerical error does make a contribution to the overall dissipation of turbulent energy. The sensitivity of the point of transition is demonstrated to be highly dependent on the coupling of the stress and flux models, and that this shows the need for accurate modelling, particularly for the flux terms.

Figure 6 shows a segment of the temperature decay in the transitional region from  $2 < y/D < 4$ . The interesting point is that it is the SGDH model simulation which has started to decay first, and subsequently goes through transition more slowly, and out of the boundaries of the plot has the highest decay again. This effect, not seen with the GGDH model, is due to the structural nature of the model.

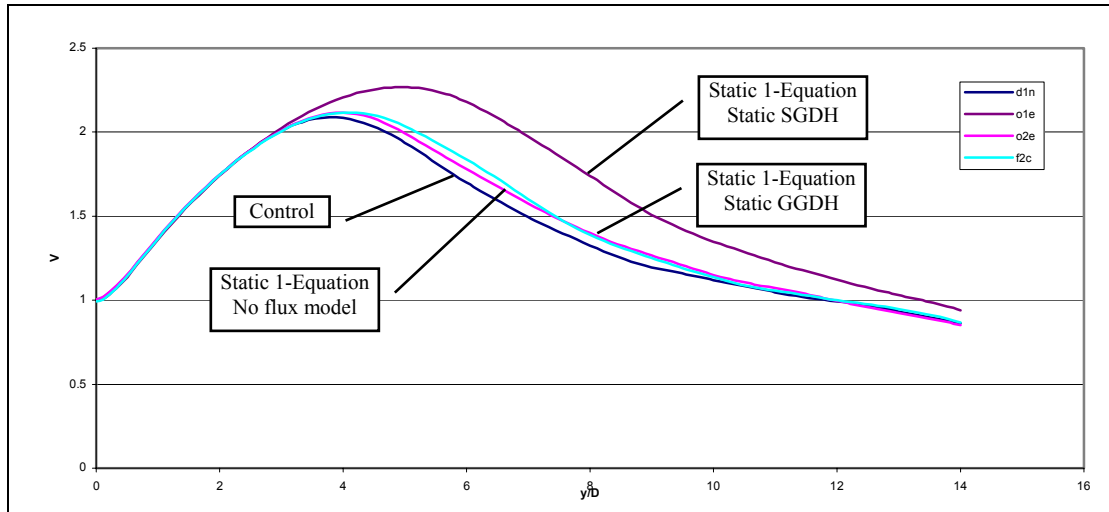


Figure 5. Velocity decay along plume centreline.

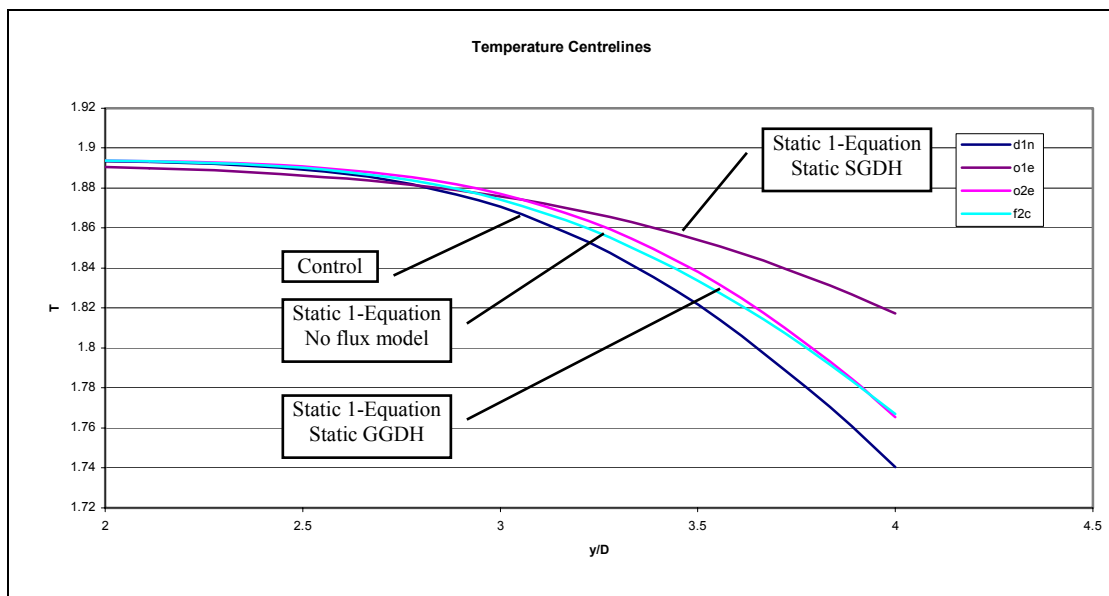


Figure 6. Temperature decay along plume centreline.

The SGDH model employs an isotropic turbulent eddy viscosity, whereas this is not the case for the GGDH model, although both are purely diffusive terms. The consequence of this is that the SGDH model incorrectly represents large laminar gradients, as found at the edge of the jet near the inlet. The model recognises this gradient as turbulence and consequently introduces significant horizontal diffusion. Similarly to the Smagorinsky model, in the SGDH model it is the radial fluxes which have the greater magnitude at their peak. The GGDH model does not connect each temperature gradient to this isotropic turbulent viscosity, but to the relevant components of the stresses, and thereby avoids this unwanted early diffusion. The effect is found everywhere, however, in that the relation between the fluxes is different for the GGDH model. The vertical flux is the dominant term everywhere, not just on the centreline. This structural difference is critical in the models. With the constants used, the SGDH model still has higher magnitudes generally, although this can clearly be altered.

Regardless, the SGDH model strongly affects the transition period adversely, through the erroneous early spread of the temperature field, the interaction of which at the transition point with the velocity field is shown to be highly sensitive, as experimentally and theoretically found by Pera and Gebhart [27].

These static Smagorinsky sub-grid model with either the SGDH or GGDH flux models show significant differences in their averaged values, largely due to their effect on transition. The dynamic models, based on the Germano relation [21], alleviate some of these problems, notably in the laminar and transitional regions, although do not overcome all the problems of a sub-grid model, most notably of backscatter, despite initial hopes to overcome this problem.

Simulations using the dynamic Smagorinsky and the static and dynamic SGDH models have been obtained and are presented below. The velocity and temperature centrelines are rather similar to the control solution, although a faster transition and larger spread rate can be observed.

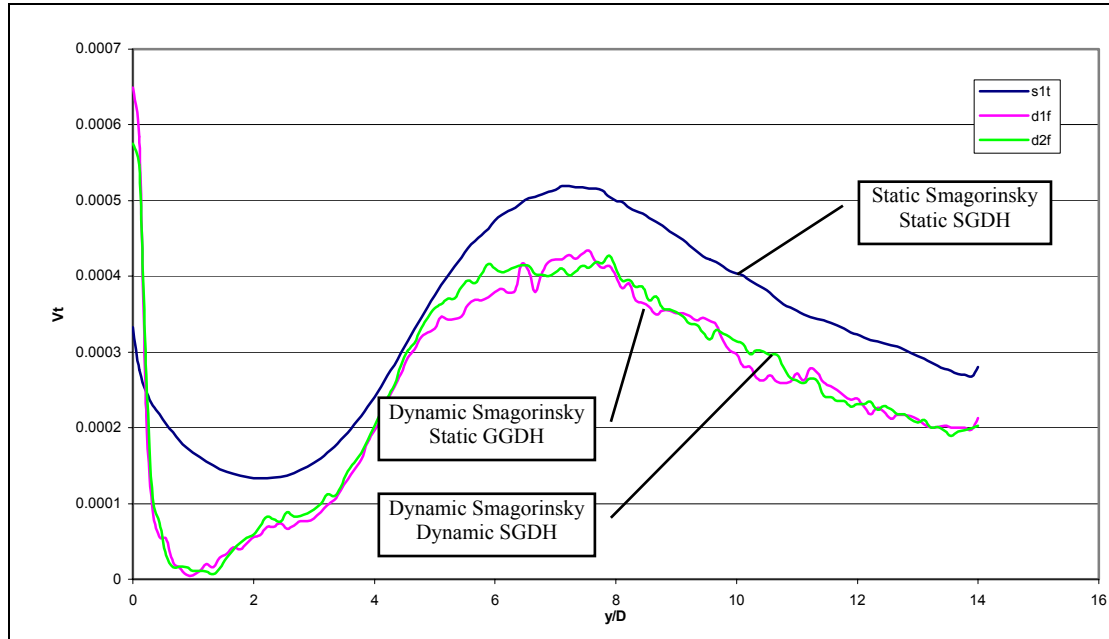


Figure 7. Turbulent viscosity centreline profile.

Figure 7 shows the centreline turbulent viscosities. A high initial value shows the instabilities caused at the inlet are quickly damped, after which the turbulent viscosity becomes negligible briefly in the laminar region, before increasing through the transition period, and later decaying along the developed plume. The turbulent viscosity is a core component of the SGDH model, and consequently the dynamic procedure is indirectly affecting the flux model also, and the dissipative effect is reduced, allowing slightly earlier transition. The dynamic Smagorinsky model is structurally the same as the static eddy models, although the erratic behaviour of the constant appears to cause extra instability in the flow, aiding transition.

The backscatter, or negative turbulent viscosity, which the dynamic technique allows for, and is requisite for accurate stress modelling Piomelli et al. [28], is necessarily numerically unstable unless the period of being negative is bounded Lund et al. [29] and consequently must be clipped. Piomelli et al. [28] find that somewhat less than 50% of the points are clipped in channel flow with a top-hat filter (this value varies with the filter type). In the developed plume region, on the centreline, averaging the points in time, rather than space, and also with a top-hat filter 30-35% of the points were clipped. It is desirable to have a model in which this value tends to zero. An instantaneous snapshot of the dynamic constant is shown in Figure 8. The distribution is seen to behave erratically in the boundary regions, and is due to numerical error, induced by very small denominators. These do not adversely affect the stress model evaluations, as the gradient components are small enough to quash these effects overall, as shown in Figure 9, of the averaged turbulent viscosity.

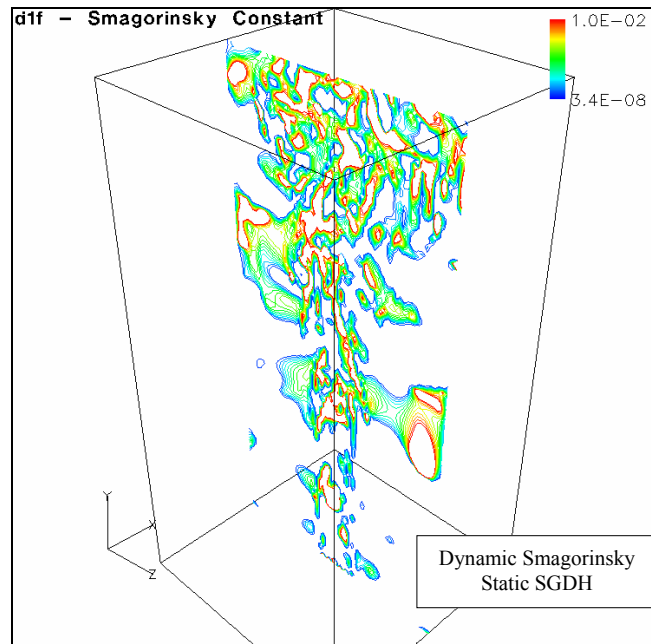


Figure 8. Instantaneous dynamic Smagorinsky model constant

The average value of the constant was found to be 0.008, approximately 20% less than the recommended value. This can be attributed to the diffusive numerical scheme, and supports the notion that the model can adjust itself to suit the numerical procedure, Jimenez [30].

The dynamic stress models are hence recommended for use over their static counterparts, although the computational cost can be prohibitive, through memory requirements, rather than an excessively high operation count. Further, test simulations with central convection schemes suggest that dynamic models can be used in cases where static models are not sufficient to dissipate sufficient energy quickly enough.

The dynamic SGD model has a greater proportion of its points clipped, approximately 45% on the turbulent centreline. This gives enough points to expect good values for the fluxes. The values are negligible, however, with the turbulent Prandtl number evaluated between one and two orders of magnitude higher than expected. This is attributed to a lack of correlation between the turbulent viscosity and the temperature fluctuations after the dynamic procedure has been used firstly to evaluate the turbulent viscosity. This implies that for the dynamic procedure to be used effectively for a flux model, a new strategy should be developed, which does not link the dynamic procedures.

## CONCLUDING REMARKS

Large eddy simulations have been carried out on thermal plumes in order to investigate the behaviour of different LES models, and to refute the argument that the choice of LES model does not matter. The static models show very apparent differences; most significantly through the flux model at the point of transition, and most importantly that the flux models are not satisfactory, although further development of the GGDH model is promising. The dynamic SGD model in these simulations is found to be numerically problematic, and a resolution to this should be found. The benefits of the dynamic models are apparent from the dynamic Smagorinsky model, and should be utilised in the fluxes as well when possible. In contrast to the statistical turbulence models in a RANS approach, the sub-grid scale model is, by definition, grid dependent. Therefore when only relatively coarse grids are employed the SGS model plays a significant role as demonstrated in this work. The expectation remains, that as available computer resources increase and finer grids are employed for fire simulations, the differences between the SGS models will become less apparent. Evidence for this remains to be demonstrated in the context of the simulation of buoyant plumes and smoke movement.

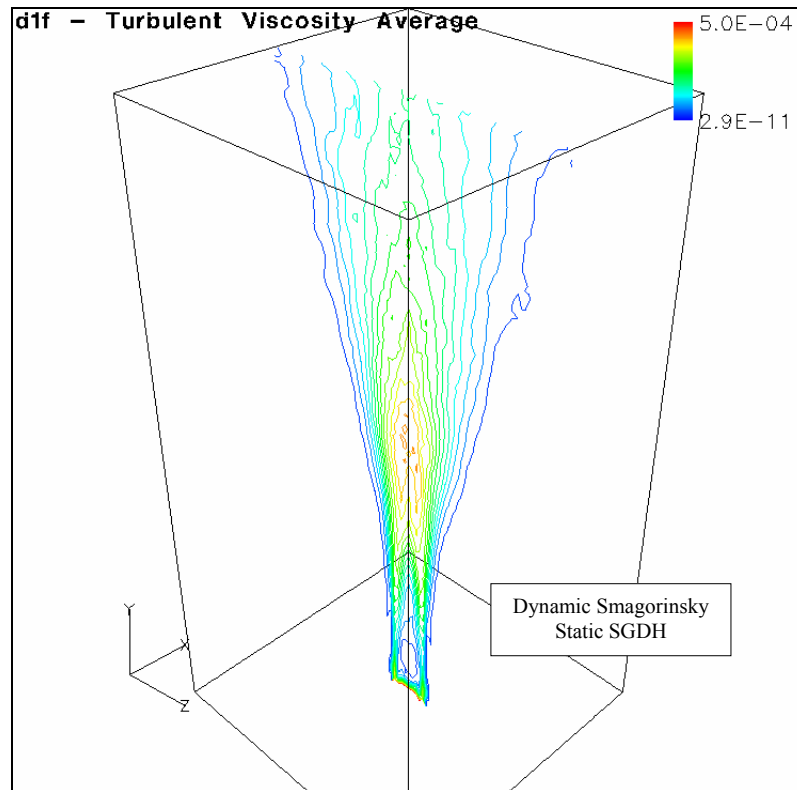


Figure 9. Average turbulent viscosity

## REFERENCES

1. Smagorinsky, J., General circulation experiments with the primitive equations, *Mon. Weather Rev.*, 91, p99, 1963.
2. Lilly, D. K., On the numerical simulation of buoyant convection, *Tellus*, XIV(2), p144, 1962.
3. Lilly, D. K., The Representation of Small-Scale Turbulence in Numerical Simulations, *IBM Scientific Computer Symposium on Environmental Sciences*, p195, 1967.
4. Deardorff, J. W., A numerical study of three-dimensional turbulent channel flow at large Reynolds numbers, *J. Fl. Mech.*, 41(2), p453, 1970.
5. Schumann, U., Subgrid-scale model for finite-difference simulations in plane channels and annuli, *J. Comp. Phys.*, 18, p376, 1975.
6. Leonard, A., Energy cascade in large-eddy simulations of turbulent flows, *Adv. Geophys.*, 18, p237, 1977.
7. Zang, Y., Street, R. L., & Koseff, J. R., A dynamic mixed subgrid-scale model and its application to turbulent recirculating flows, *Phys. Fluids A*, 5(12), p3186, 1993.
8. Cottet, G.-H., & Vasilyev, O. V., Comparison of dynamic Smagorinsky and anisotropic subgrid-scale models, *Proc. Summer Program, Centre of Turbulence Research, Stanford*, 1998.
9. Bastiaans, R. J. M., Rindt, C. M. M., Nieuwstadt, F. T. M. & van Steenhoven, A. A., Direct and large-eddy simulation of the transition of two- and three-dimensional plumes in a confined enclosure, *I. J. Heat Mass Trans.*, 43, p2375, 2000.
10. Peng, S.-H., & Davidson, L., Large eddy simulation for turbulent buoyant flow in a confined cavity, *Int. J. Heat Fluid Flow*, 22, p323, 2001.

11. Rehm, R. G. & Baum, H. R., The Equations of Motion for Thermally Driven, Buoyant Flows, *J. Res. Nat. Bur. Stand.*, 83, p297, 1978.
12. Paulucci, S., On the Filtering of Sound from the Navier-Stokes Equations, Sandia National Labs, Report SAND-82-8257, 1982.
13. Germano, M., Turbulence: the filtering approach, *J. Fluid Mech.*, 238, p325, 1992.
14. Horiuti, K., Large Eddy Simulation of Turbulent Channel Flow by One-Equation Modelling, *J. Phys. Soc. Jap.*, 54(8), p2855, 1985.
15. Sagaut, P., Large Eddy Simulation for Incompressible Flows: An Introduction, Springer-Verlag, Berlin, 2000.
16. Schmidt H., & Schumann, U., Coherent Structure of the Convective Boundary Layer Derived from Large-Eddy Simulations, *J. Fl. Mech.*, 200, p511, 1989.
17. Davidson, Lars, A Note on Derivation of the Equations for the Subgrid Turbulent Kinetic Energies, Rep. 97/12, Dept. of Thermo and Fluid Dynamics, Chalmers University of Technology, 1997a.
18. Daly, B. J., & Harlow, F. H., Transport Equations in Turbulence, *Phys. Fluids*, 13(11), p2634, 1970.
19. Sanderson, V. E., Turbulence Modelling of Turbulent Buoyant Jets and Compartment Fires, PhD Thesis, Cranfield University, 2001.
20. Worthy, J., Sanderson, V., & Rubini, P. A., Comparison of Modified k- $\epsilon$  Turbulence Models for Buoyant Plumes, *Num. Heat Transfer, Part B*, 39, p151, 2001.
21. Germano, M., Piomelli, U., Moin, P., & Cabot, W. H., A dynamic subgrid-scale eddy viscosity model, *Phys. Fluids A*, 3(7), p1760, 1991.
22. Lilly, D. K., A proposed modification of the Germano subgrid-scale closure method, *Phys. Fluids A*, 4(3), p633, 1992.
23. Najm, H.N., Wyckoff, P.S., & Knio, O.M., A Semi-Implicit Numerical Scheme for Reacting Flow. I. Stiff Chemistry, *J. Comp. Phys.*, 143(2), p381, 1998.
24. Sweby, P. K., High Resolution Schemes using Flux Limiters for Hyperbolic Conservation Laws, *SIAM J. Numer. Anal.*, 21(5), p995, 1984.
25. Shabbir, A. & George, W. K., Experiments on a round turbulent buoyant plume, *J. Fluid. Mech.*, 275, p1, 1994.
26. Zhou, X., Luo, K. H., & Williams, J. J. R., Large-eddy simulation of a turbulent forced plume, *Eur. J. Mech. B – Fluids*, 20, p233, 2001.
27. Pera, L. & Gebhart, B., On The Stability Of Laminar Plumes: Some Numerical Solutions And Experiments, *Int. J. Heat Mass Transfer*, 14, p975, 1971.
28. Piomelli, U., Cabot, W. H., Moin, P., & Lee, S., Subgrid-scale backscatter in turbulent and transitional flows, *Phys. Fluids A*, 3(7), p1766, 1991.
29. Lund, T. S., Ghosal, S., & Moin, P., Numerical experiments with highly variable eddy viscosity models, in *Engineering Applications of Large Eddy Simulation*, eds. Ragale, S. A., & Piomelli, U., FED Vol. 162, ASME, 1993.
30. Jimenez, J., On why dynamic subgrid-scale models work, Annual Research Briefs, Centre for Turbulence Research, NASA Ames/Stanford Univ., 1995.
31. Ghosal, S., Lund, T. S., Moin, P., & Akselvoll, K., A dynamic localization model for large-eddy simulation of turbulent flows, *J. Fluid Mech.*, 286, p229, 1995.